

Monopolium production from photon fusion at the Large Hadron Collider

Luis N. Epele^a, Huner Fanchiotti^a, Carlos A. García Canal^a
and Vicente Vento^{b,c}

(a) *Laboratorio de Física Teórica, Departamento de Física, IFLP
Facultad de Ciencias Exactas, Universidad Nacional de La Plata
C.C. 67, 1900 La Plata, Argentina.*

(E-mail: epele@fisica.unlp.edu.ar, garcia@fisica.unlp.edu.ar, huner@fisica.unlp.edu.ar)

(b) *Departamento de Física Teórica and Instituto de Física Corpuscular
Universidad de Valencia and Consejo Superior de Investigaciones Científicas
E-46100 Burjassot (Valencia), Spain*

(E-mail: Vicente.Vento@uv.es)

(c) *TH-Division, PH Department, CERN
CH-1211 Genève 23, Switzerland*

Abstract

Magnetic monopoles have attracted the attention of physicists since the founding of the electromagnetic theory. Their search has been a constant endeavor which was intensified when Dirac established the relation between the existence of monopoles and charge quantization. However, these searches have been unsuccessful. We have recently proposed that monopolium, a monopole-antimonopole bound state, so strongly bound that it has a relatively small mass, could be easier to find and become an indirect but clear signature for the existence of magnetic monopoles. In here we extend our previous analysis for its production to two photon fusion at LHC energies.

Pacs: 14.80.Hv, 95.30.Cq, 98.70.-f, 98.80.-k

Keywords: partons, photons, monopoles, monopolium,

1 Introduction

The theoretical justification for the existence of classical magnetic poles is that they add symmetry to Maxwell's equations and explain charge quantization [1, 2, 3]. Dirac formulated his theory of monopoles considering them point-like particles and quantum mechanical consistency conditions lead to the so called Dirac Quantization Condition (DQC),

$$e g = \frac{N}{2}, \quad N = 1, 2, \dots, \quad (1)$$

where e is the electron charge, g the monopole magnetic charge and we use natural units $\hbar = c = 1$.

Numerous experimental searches for monopoles have been carried out but all have met with failure [4, 5, 6, 7, 8, 9, 10]. The last, carried out by the CDF collaboration at the Fermi National Laboratory [11], found no monopoles and established a lower mass limit of 360 GeV.

This lack of experimental confirmation has led many physicists to abandon the hope in their existence. A way out of this impasse is the old idea of Dirac [1, 12], namely, monopoles are not seen freely because they are confined by their strong magnetic forces forming a bound state called monopolium [13, 14]. This idea was the leitmotiv behind our recent research [15], namely we proposed that monopolium might be easier to detect than free monopoles. We showed that certain parameterizations of the mass and the width, allowed for such a scenario.

The Large Hadron Collider (LHC) will soon enter in operation and will probe the new energy frontier opening possibilities for new physics including the discovery of magnetic monopoles either directly, a possibility contemplated long time ago, [16, 17], or through the discovery of monopolium, as we have been advocating. This development motivates our present research which analyzes the production of monopolium at LHC by the mechanism of photon fusion.

Recently, Dougall and Wick have presented a calculation of monopole–antimonopole production from photon fusion at proton colliders [18, 19]. The mass limit of CDF was obtained assuming Drell-Yan (DY) production which dominates over other processes at Tevatron energies. Dougall and Wick have shown that at LHC energies photon fusion is the dominant process [18, 19]. We proceed to calculate the production of monopolium by means of this process and compare our results with monopole–antimonopole production. We conclude that, if monopolium is a strongly bound state, its cross section is larger than that for creating a heavy monopole-antimonopole pair and consequently gives rise to a more clear experimental signal.

2 Monopolium production

A useful computational theory of monopoles does not currently exist to perform a direct production calculation. For this reason we will employ a minimal model of monopole inter-

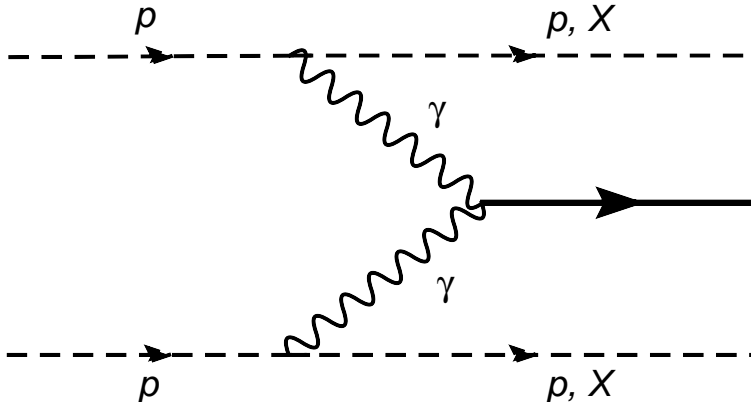


Figure 1: Diagrammatic description of the reaction studied.

action which assumes a monopole photon-coupling which is proportional to the monopole's induced electric field $g\beta$ for a monopole moving with velocity β [18, 19, 20]. This approximation can be shown to be almost equivalent to the low energy effective theory of Ginzburg and Schiller [21, 22]. This theory was derived from the standard electroweak theory in the one loop approximation leading to an effective coupling proportional to $g_{eff} \sim \frac{\omega}{m} g$, where ω is a kinematical energy scale of the process which is below the monopole production threshold, thus rendering the theory perturbative. This is so because that in a photon fusion diagram the dynamical scale is $\sqrt{E^2 - 4m^2}$, thus

$$\frac{\omega}{m} \sim \frac{\sqrt{E^2 - 4m^2}}{2m} \sim \frac{E\beta}{2m}, \quad (2)$$

and therefore if $E \sim 2m$, i.e., kinetic terms are small, both schemes coincide. Here ω describes the active energy scale, E the center of mass energy, m the monopole mass and β the velocity.

The Dirac quantization condition does not specify the spin of the monopoles. We choose here monopoles of spin 1/2, following Dougall and Wick [18, 19], coupled in monopolum to spin 0 in order to have a minimum energy radial structure.

We then study the expected production process at LHC, namely

$$p + p \rightarrow p(X) + p(X) + M, \quad (3)$$

shown in Fig.1, where p represents the proton, X an unknown final state and M the monopolum. This diagram summarizes the three possible processes:

- i) inelastic $p + p \rightarrow X + X + (\gamma\gamma) \rightarrow X + X + M$
- ii) semi-elastic $p + p \rightarrow p + X + (\gamma\gamma) \rightarrow p + X + M$
- iii) elastic $p + p \rightarrow p + p + (\gamma\gamma) \rightarrow p + p + M$.

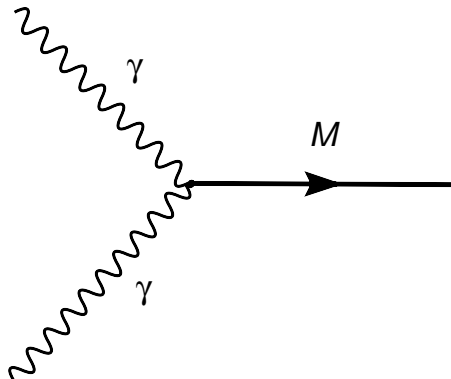


Figure 2: Diagrammatic description of the elementary subprocess of the monopodium production from photon fusion.

In the inelastic scattering, both intermediate photons are radiated from partons (quarks or antiquarks) in the colliding protons.

In the semi-elastic scattering one intermediate photon is radiated by a quark (or antiquark), as in the inelastic process, while the second photon is radiated from the other proton, coupling to the total proton charge and leaving a final state proton intact.

In the elastic scattering both intermediate photons are radiated from the interacting protons leaving both protons intact in the final state.

The full $\gamma\gamma$ calculation includes contributions from these three individual regimes.

We next proceed to describe the elementary subprocess shown in Fig. 2, which deals only with photons and monopodium, and will come back to the full pp scattering treatment later on. The standard expression for the cross section of this elementary subprocess results in

$$\sigma(2\gamma \rightarrow M) = \frac{4\pi}{E^2} \frac{M^2 \Gamma(E) \Gamma_M}{(E^2 - M^2)^2 + M^2 \Gamma_M^2} \quad (4)$$

where we have assumed that monopodium decays with a width Γ_M and $\Gamma(E)$, with E off mass shell, describes the production cross section. The width Γ_M arises from the softening of a delta function, $\delta(E^2 - M^2)$ and therefore is, in principle, independent of the production rate $\Gamma(E)$ [23].

We enter now the computation of the $\Gamma(E)$, which represents the width of the 2γ decay of monopodium. The calculation, following standard field theoretic techniques of the decay of a non-relativistic bound state [23, 24], leads to

$$\Gamma(E) = \frac{32\pi\alpha_g^2}{M^2} |\psi_M(0)|^2. \quad (5)$$

We have used the conventional approximations, namely that the monopoles are almost on shell and that in the calculation of the elementary process we have neglected the binding energy, i.e. $M = 2m$. However, we express the final formula in terms of the monopodium

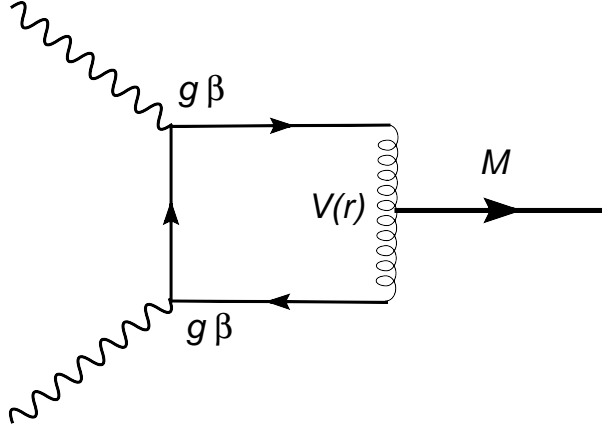


Figure 3: Diagrammatic representation of the model describing the coupling of photons to monopolum.

mass, M , because the latter will take care of the binding. Here α_g corresponds to the photon–monopole coupling and ψ_M is the monopolum ground state wave function.

Using the Coulomb wave functions of ref.[15] expressed in the most convenient way to avoid details of the interaction, which will be parameterized by the binding energy, one has

$$|\psi_M(0)|^2 = \frac{1}{\pi} \left(2 - \frac{M}{m}\right)^{3/2} m^3, \quad (6)$$

and the scheme of Dougall and Wick [18, 19] adapted to monopolum production, gives rise to

$$\Gamma(E) = \frac{2\beta^4}{M^2 \alpha^2} \left(2 - \frac{M}{m}\right)^{3/2} m^3. \quad (7)$$

Here, α is the fine structure constant and β the monopolum velocity,

$$\beta = \sqrt{1 - \frac{M^2}{E^2}}. \quad (8)$$

which is the velocity of the monopoles moving in the monopolum system.

Note that due to the value of β the width vanishes at the monopolum mass, where the velocity is zero. Therefore a static monopolum is stable under this interaction.

A caveat must be made. There is a duality of treatments in the above formulation, see Fig. 3. The static coupling is treated as a Coloumb like interaction of coupling g binding the monopoles into monopolum, although ultimately the details are eliminated in favor of the binding energy parameterized by the monopolum mass M . We find in this way a simple parametric description of the bound state. The dynamics of the production of the virtual monopoles, to be bound in monopolum, is described in accordance with the effective theory [18, 19], and this coupling is βg . This is similar to what is done in heavy quark physics [25](see his figure 5), where the wave function is obtained by a

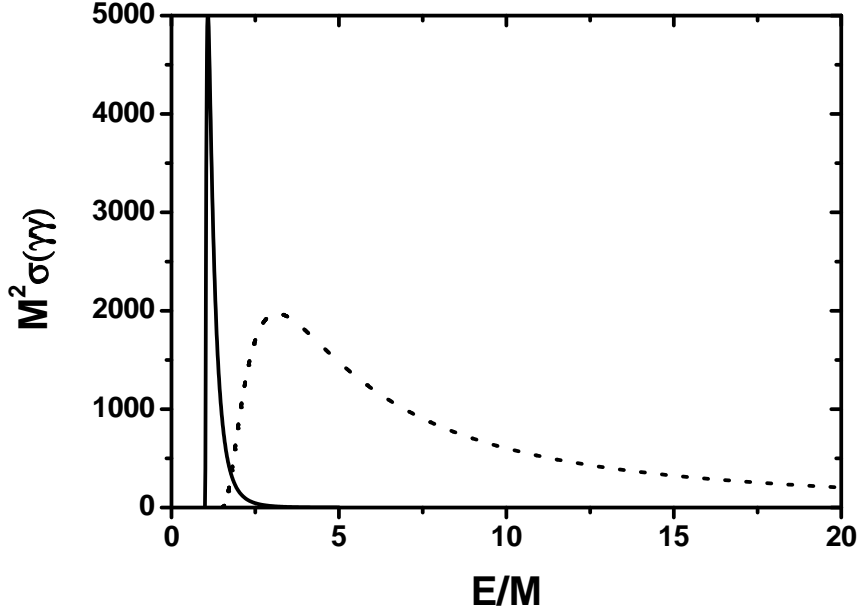


Figure 4: We show the photon fusion production cross section for monopolum (solid curve) for $R = 1.5$ and $\bar{\Gamma}_M = 0.1$, and for monopole-antimonopole (dotted curve) as a function of the energy variable $\mathcal{E} = E/M$.

parametric description using approximate strong dynamics while the coupling to photons is elementary.

The production cross section can now be written as

$$M^2\sigma(2\gamma \rightarrow M) = \frac{2\sqrt{2}\pi R^{3/2}(R-1)^{1.5}}{\alpha^2 \mathcal{E}^6} \frac{\bar{\Gamma}_M(\mathcal{E}^2 - 1)^2}{(\mathcal{E}^2 - 1)^2 + \bar{\Gamma}_M^2}, \quad (9)$$

where $R = 2m/M$, ($1 < R < \infty$). This parameter ratio describes the binding energy of monopolum in units of M , since $M = 2m + E_{binding}$. $\mathcal{E} = E/M$ is the center of mass energy measured in units of M and $\bar{\Gamma}_M = \Gamma_M/M$ is the decay width of monopolum also measured in units of M . The right hand side is adimensional and therefore the above expression gives the cross section in units of $1/M^2$. The monopolum width, which vanishes with our dynamics, arises from higher order effects or other possible dynamics and we consider it as a parameter. Even in the case monopolum would be stable at rest the width would parameterize the beam width [23].

In Fig. 4 we show the photon fusion cross section for monopolum for a value of $R = 1.5$ and $\bar{\Gamma}_M = 0.1$, together with that for monopole-antimonopole obtained in ref. [18, 19], which we have simply rewritten using M as the energy unit,

$$M^2\sigma(2\gamma \rightarrow M) = \frac{\pi R^2 (1 - \beta'^2)\beta'^5}{14\alpha^2 m^2} \left(\frac{3 - \beta'^4}{2\beta'} \log \left(\frac{1 + \beta'}{1 - \beta'} \right) - (2 - \beta^2) \right), \quad (10)$$

where $\beta' = \sqrt{1 - \frac{4m^2}{E^2}}$.

The qualitative features of both cross sections are radically different. The monopolium cross section is a spike slightly above the monopolium mass, where it vanishes, assuming a reasonable width $\Gamma_M < M$, while the monopole-antimonopole cross section is a soft curve extending over a large energy region. It is also clear from Eq. (9) that the height of the pick strongly depends on the value of the binding, i.e., the larger the binding energy the larger will be R and the higher will be the pick.

It is important to note that the approach followed to describe the coupling ($g \rightarrow g\beta$) provides us with a large negative power of energy which makes the monopolium cross section fall off very rapidly. In the Ginzburg-Schiller approach, four powers of the energy are substituted by four powers of the monopolium mass and therefore one obtains a larger effective width for the pick, and thus a larger integrated cross section for the same values of R and $\bar{\Gamma}_M$.

3 Cross section estimates

We calculate $\gamma\gamma$ fusion for monopolium production following the formalism of Drees et al. [26] benefitting from the the full documentation of the calculation in the work of Dougall and Wick [18, 19]. We obtain therewith the pp cross section for monopolium and for monopole-antimonopole production within the same computational codes.

The full pp calculation includes contributions of three types: inelastic, semi-elastic, and elastic scattering. We sum these individual contributions to find the total pp cross-section, σ_{tot} .

In the inelastic scattering, $p + p \rightarrow X + X + (\gamma\gamma) \rightarrow X + X + M$, to approximate the quark distribution within the proton we use the Cteq6-1L parton distribution functions [27] and choose $Q^2 = \hat{s}/4$ throughout.

We employ an equivalent-photon approximation for the photon spectrum of the intermediate quarks [28, 29].

In semi-elastic scattering, $p + p \rightarrow p + X + (\gamma\gamma) \rightarrow p + X + M$, the photon spectrum associated with the interacting proton must be altered from the equivalent-photon approximation for quarks to account for the proton structure. To accommodate the proton structure we use the modified equivalent-photon approximation of [30].

For elastic scattering, $p + p \rightarrow p + p + (\gamma\gamma) \rightarrow p + p + M$, both protons remain intact in the final state.

In Fig.5 we show the comparison between monopole-antimonopole and monopolium production cross sections using M as energy unit as a function of $R = 2m/M$, i.e., binding energy $|E_{binding}|/M = R - 1$. Two regimes are found:

- i) the low binding regime $1 < R < 2$ where the $m\bar{m}$ production is dominant;
- ii) the large binding regime $R > 2$ where monopolium production is dominant and can be very large.

In Fig.6 we plot the logarithm of the total cross section (in fb) for pp production of monopolium as a function of monopole mass, for two masses of monopolium ($M=100$

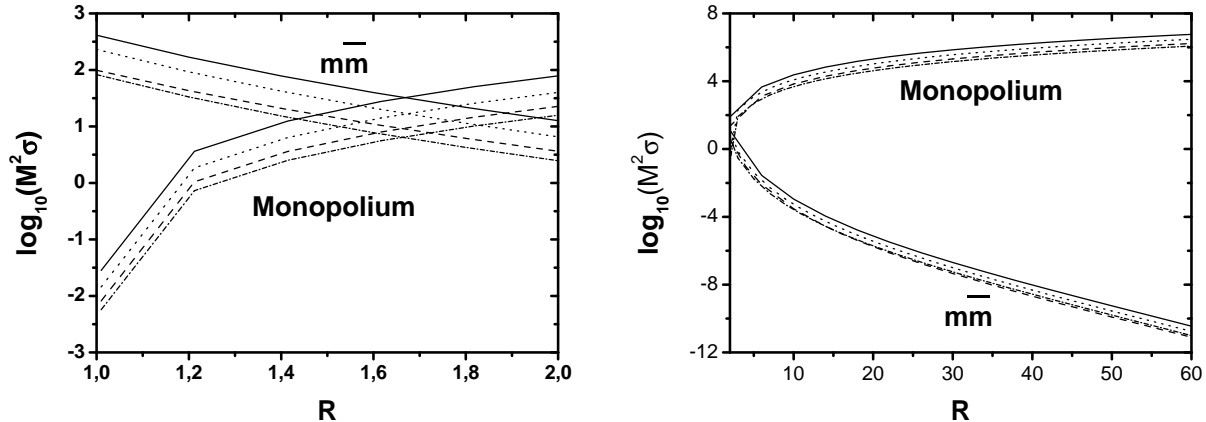


Figure 5: The left figure shows logarithmic plots of the pp production cross sections (in units of M^2) via photon fusion for monopoliium ($\Gamma_M = 0.1M$) and for monopole-antimonopole as a function $R = 2m/M$ for low binding. The figure on the right shows logarithmic plots of the pp production cross section (in units of M^2) via photon fusion for monopoliium ($\Gamma_M = 0.1M$) and for monopole-antimonopole as a function of R for large binding. The solid line represents the total cross section; the various contributions are represented by: inelastic (dashed line); semielastic (dotted line) and elastic (dot-dashed line).

GeV and $M = 1000$ GeV), as well as the total cross section for monopole-antimonopole production as a function of monopole mass. The two mass plot shows the dependence with monopoliium mass of the cross section. There is always a threshold at $m = M/2$, i.e. for zero binding energy, where the cross section vanishes, and then a rapid rise with monopole mass. Thereafter the cross section grows in a softer manner, although it should be realized that we deal with a log plot and therefore the growth is not negligible. Finally, the smaller the monopoliium mass, the larger the cross section is.

The most spectacular signature of the curves is that for fixed monopoliium mass the cross section increases with monopole mass, instead of decreasing, as happens in monopole-antimonopole production, and the magnitude becomes enormous for very large binding energy. Thus a strongly bound monopoliium state would be an ideal system to disentangle monopole dynamics.

4 Conclusions

We have carried out an investigation looking for hints of the so far not seen monopoles. Our motivation has been, that of our previous work [15], namely that monopoliium, if strongly bound, is easier to produce than monopole-antimonopole pairs.

We have performed a calculation in which monopoliium is produced via the conventional monopole dynamics [18, 19] used to study monopole-antimonopole production by photon fusion at LHC energies. Our calculation is parameterized in terms of three quantities: m , the monopole mass, M the monopoliium mass (or binding energy) and the width

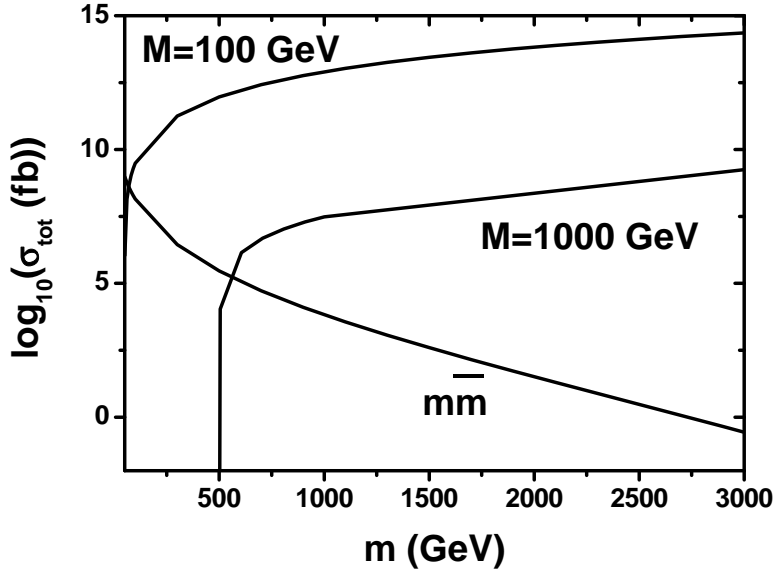


Figure 6: We represent the logarithmic plot of the total pp cross section from photon fusion in femtobarns as a function of monopole mass, for two monopolum masses $M = 100$ GeV and $M = 1000$ GeV and compare it with the corresponding monopole-antimonopole ($m \bar{m}$) cross section.

Γ_M which we simply take to be narrow compared with the monopolum mass.

Our analysis distinguishes two clearly distinct regions associated with the binding energy in monopolum. If the binding energy is small compared to the monopole mass, the monopole-antimonopole process will be dominant. On the contrary if it is comparable or larger, the monopolum process is not only dominant but can be extremely large.

The most favorable scenario, which agrees with that discussed in our previous work, is a two energy scale scenario, whose

- i) low energy scale is governed by the monopolum mass, M , reachable by LHC,
- ii) and whose high energy scale is governed by the monopole mass, m , which arises through the structure of monopolum, and which could be larger than the energy reachable by LHC.

Under these circumstances the cross section as a function of the monopole mass becomes sizeable.

An example, if monopole and monopolum have a mass of 1 TeV, at an integrated luminosity of 100 fb^{-1} at LHC, Dougall and Wick predict about 10^6 monopoles, while our calculation would produce 10^8 monopolia.

Since at present we cannot calculate the monopolum parameters, M and Γ_M , the experimental endeavor is not easy. However, if we extend the theory to incorporate the weak interaction [21, 22] there are some features which might simplify the task,

- i) the resonance peak of the monopolium can be found in three exit channels 2γ , γZ_0 and $2 Z_0$'s.
- ii) monopolium can be produced in an excited state before it annihilates, thus the annihilation process will be accompanied by a Rydberg radiation spectrum;

The calculated values for the cross sections, corresponding to reasonable monopolium mass scenarios, render our calculation sound and this line of research worth pursuing.

Acknowledgement

We thank the authors of JaxoDraw for making drawing diagrams an easy task [31]. This work was done while one of us (VV) was on a sabbatical from the University of Valencia at the PH-TH at CERN, whose members he thanks for their hospitality. VV was supported by MECyT-FPA2007 and by MEC-Movilidad PR2007-0048. LNE, HF and CAGC were partially supported by CONICET and ANPCyT Argentina.

References

- [1] P. A. M. Dirac, Proc. Roy. Soc. Lond. A **133** (1931) 60.
- [2] P. A. M. Dirac, Phys. Rev. **74** (1948) 817.
- [3] J. D. Jackson, Classical Electrodynamics, de Gruyter, N.Y. (1982).
- [4] N. Craigie, G. Giacomelli, W. Nahern and Q. Shafi, Theory and detection of magnetic monopoles in gauge theories, World Scientific, Singapore 1986.
- [5] G. Giacomelli and L. Patrizzii, arXiv:hep-ex/0506014.
- [6] P.D.B. Martin Collins, A.D. Martin and E.J. Squires, Particle Physics and Cosmology, Wiley, N.Y. (1989)
- [7] K. A. Milton, Rept. Prog. Phys. **69** (2006) 1637 [arXiv:hep-ex/0602040].
- [8] S. Eidelman *et al.* [Particle Data Group], Phys. Lett. B **592** (2004) 1.
- [9] W. M. Yao *et al.* [Particle Data Group], J. Phys. G **33** (2006) 1.
- [10] M. J. Mulhearn, "A direct search for Dirac magnetic monopoles," Fermilab-Thesis-2004-51.
- [11] A. Abulencia *et al.* [CDF Collaboration], Phys. Rev. Lett. **96** (2006) 201801 [arXiv:hep-ex/0509015].
- [12] Y. B. Zeldovich and M. Y. Khlopov, Phys. Lett. B **79** (1978) 239.

- [13] C. T. Hill, Nucl. Phys. B **224** (1983) 469.
- [14] V. K. Dubrovich, Grav. Cosmol. Suppl. **8N1** (2002) 122.
- [15] L. N. Epele, H. Fanchiotti, C. A. Garcia Canal and V. Vento, Eur. Phys. J. C **56** (2008) 87 [arXiv:hep-ph/0701133].
- [16] I. F. Ginzburg, G. L. Kotkin, V. G. Serbo and V. I. Telnov, Nucl. Instrum. Meth. **205** (1983) 47.
- [17] I. F. Ginzburg and S. L. Panfil, Sov. J. Nucl. Phys. **36** (1982) 850 [Yad. Fiz. **36** (1982) 1461].
- [18] T. Dougall and S. D. Wick, arXiv:0706.1042 [hep-ph].
- [19] T. Dougall, “Monopole pair production via photon fusion,” Thesis Southern Methodist University December 9, 2006.
- [20] G. R. Kalbfleisch, K. A. Milton, M. G. Strauss, L. P. Gamberg, E. H. Smith and W. Luo, Phys. Rev. Lett. **85** (2000) 5292 [arXiv:hep-ex/0005005].
- [21] I. F. Ginzburg and A. Schiller, Phys. Rev. D **57** (1998) 6599 [arXiv:hep-ph/9802310].
- [22] I. F. Ginzburg and A. Schiller, Phys. Rev. D **60** (1999) 075016 [arXiv:hep-ph/9903314].
- [23] M.E. Peskin and D.V. Schroeder, An introduction to quantum field theory, (Harper-Collins, 1995).
- [24] J.M. Jauch and F. Rorhlich, The theory of electrons and photons (Springer 1975).
- [25] M. R. Pennington, Acta Phys. Polon. B **37** (2006) 857 [arXiv:hep-ph/0511146].
- [26] M. Drees, R. M. Godbole, M. Nowakowski and S. D. Rindani, Phys. Rev. D **50** (1994) 2335 [arXiv:hep-ph/9403368].
- [27] The Cteq6 parton distribution functions can be found at
[<http://www.phys.psu.edu//cteq/>].
- [28] E. J. Williams, Phys. Rev. **45** (1934) 729.
- [29] C. F. von Weizsacker, Z. Phys. **88** (1934) 612.
- [30] M. Drees and D. Zeppenfeld, Phys. Rev. D **39** (1989) 2536.
- [31] D. Binosi and L. Theussl, Comput. Phys. Commun. **161** (2004) 76 [arXiv:hep-ph/0309015].